Supporting information for

Concavity Tuning of Intermetallic Pd-Pb Nanocubes for Selective Semihydrogenation Catalysis

Junbo Zhang,[1+] Weiwei Xu,[2+] Lai, Xu,[2]* Qi Shao,[1] and Xiaoqing Huang[1]*

[1]*College of Chemistry, Chemical Engineering and Materials Science, Soochow University, Jiangsu 215123, China.*

[2]*Institute of Functional Nano & Soft Materials (FUNSOM), Jiangsu Key Laboratory for Carbon-Based Functional Materials & Devices, Soochow University, Jiangsu, 215123, China.*

Email: xulai15@suda.edu.cn; hxq006@suda.edu.cn

Experimental Procedures

1.1 DFT models and calculations: All the calculations were carried out by the "Vienna ab initio simulation package" (VASP5.4.4).[1-4] The core and valence electrons were represented by the projector augmented wave (PAW) method and plane-wave basis functions with a kinetic energy cut-off of 400 eV, and the Brillouin zone was sampled using a Gamma Monkhorst-Pack grid. The generalized gradient approximation (GGA) with Perdew-Burke-Ernzerh (PBE) functional was chosen to describe the electronic interaction effect in the calculations.[5] Ground-state atomic geometries were obtained by minimizing the energy and force to 1.0×10^{-5} eV/atom and 0.05 eV/Å. To examine the effect of van der Waals interaction on reaction energetics, calculations were performed by using the DFT-D3 functional with PBE-PAW potentials.[1,6] The vacuum spacing in the direction along Z axis, with respect to the surface was 15 Å between neighboring slab images, which is sufficient to eliminate the interactions between the slabs. The climbing image nudged elastic band (CI-NEB) method was used to search the transition states and track minimum-energy paths for the reactions.[7-8]

Reference

(1) Kresse, G.; Joubert, D. From ultrasoft pseudopotentials to the projector augmented-wave method. *Phys. Rev. B* **1999**, *59*, 1758-1775.

(2) Kresse, G.; Furthmüller, J. Efficient iterative schemes for *ab-initio* total-energy calculations using a plane-wave basis set. *Phys. Rev. B* **1996**, *54*, 11169-11186.

(3) Blöchl, P. E. Projector augmented-wave method. *Phys. Rev. B* **1994**, *50*, 17953-17979.

(4) Kresse, G.; Hafner, J. *Ab initio* molecular-dynamics simulation of the liquid-metal-amorphous-semiconductor transition in germanium. *Phys. Rev. B* **1994**, *49*, 14251-14269.

(5) Perdew, J. P.; Burke, K.; Ernzerhof, M. Generalized gradient approximation made simple. *Phys. Rev. Lett.* **1996**, *77*, 3865-3868.

(6) Grimme, S.; Antony, J.; Ehrlich, S.; Krieg, H. A consistent and accurate *ab initio* parametrization of density functional dispersion correction (DFT-D) for the 94 elements H-Pu. *J. Chem. Phys.* **2010**, *132*, 154104.

(7) Henkelman, G.; Uberuaga, B. P.; Jónsson, H. A climbing image nudged elastic band method for finding saddle points and minimum energy paths. *J. Chem. Phys*. **2000**, *113*, 9901-9904.

(8) Mills, G.; Jónsson, H.; Schenter, G.K. Reversible work transition state theory: application to dissociative adsorption of hydrogen. *Surf. Sci*. **1995**, *324*, 305-337.

Supplementary Figures and Table: Figure S1-Figure S14 and Table 1-Table 2

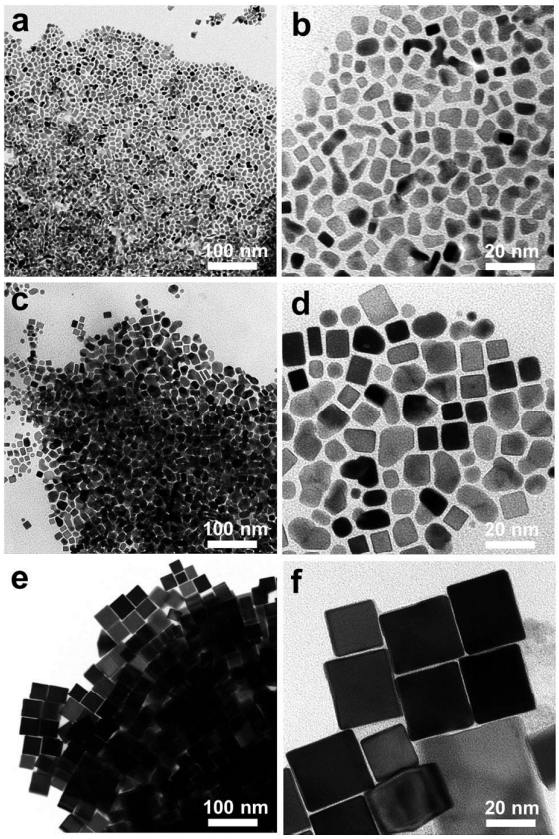

Figure S1. TEM images of the products obtained by using the same reaction conditions as those of Pd_3Pb NCs except for the use of (a, b) 0 mg DTAC, (c, d) 3.3 mg DTAC and (e, f) 26.4 mg DTAC.

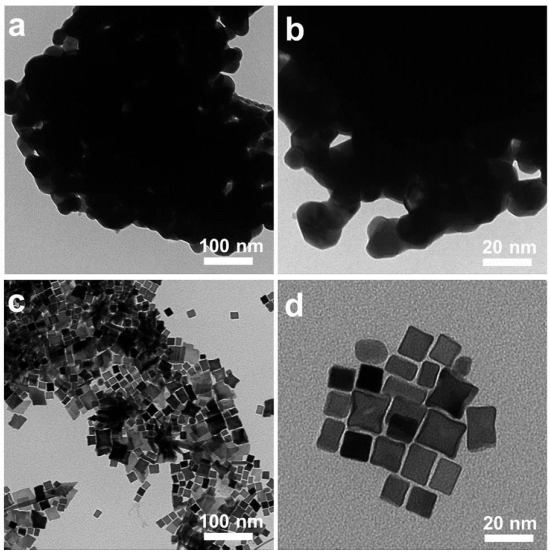

Figure S2. TEM images of the products obtained by using the same reaction conditions as those of Pd_3Pb SCNCs except for the use of (a, b) 20 mg benzoic acid and (c, d) 80 mg benzoic acid.

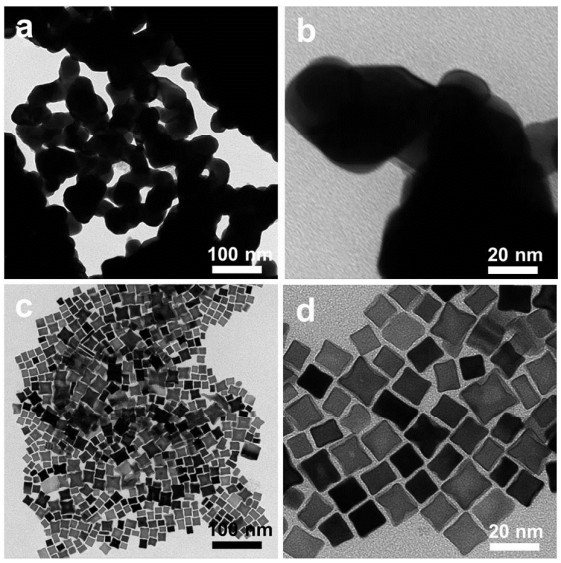

Figure S3. TEM images of the products obtained by using the same reaction conditions as those of Pd_3Pb CNCs except for the use of (a, b) 0.05 mL benzaldehyde and (c, d) 0.2 mL benzaldehyde.

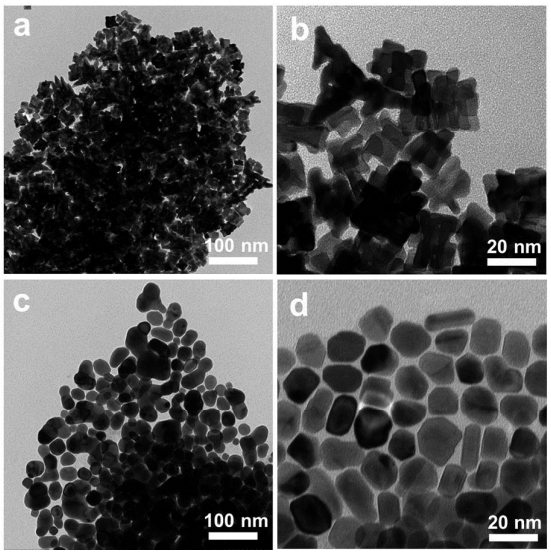

Figure S4. TEM images of the products obtained by using the same reaction conditions as those of Pd_3Pb CNCs but changing 0.1 mL benzaldehyde to (a, b) 0.1 mL benzyl alcohol and (c, d) 0.1 mL aniline.

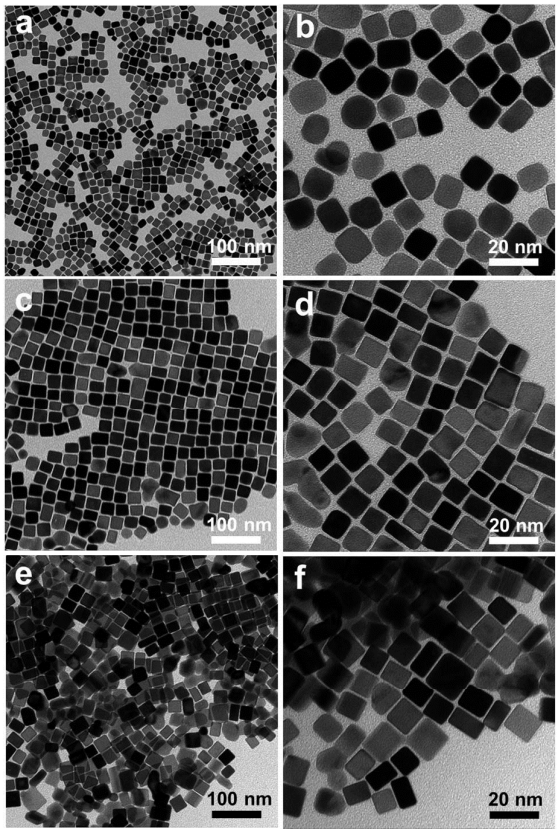

Figure S5. TEM images of the products obtained by using the same reaction conditions as those of Pd_3Pb NCs but changing 3.2 mg $Pb(Ac)_2 \cdot 3H_2O$ to (a, b) 2.3 mg $PbCl_2$, (c, d) 3.8 mg $Pb(acac)_2$ and 2.7 mg $Pb(HCOO)_2$, respectively.

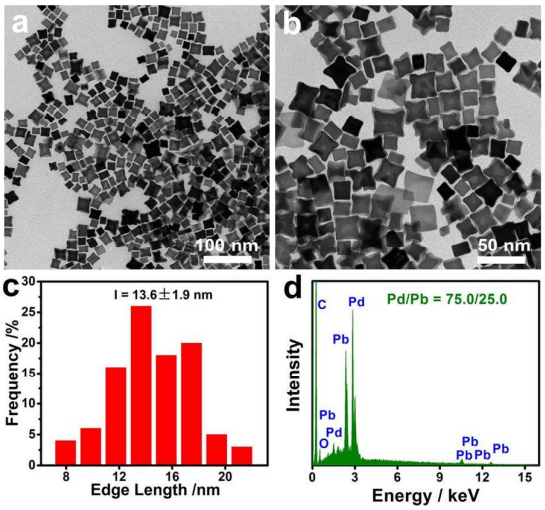

Figure S6. (a, b) TEM images, (c) edge length distribution and (d) SEM-EDX of the Pd_3Pb CNCs.

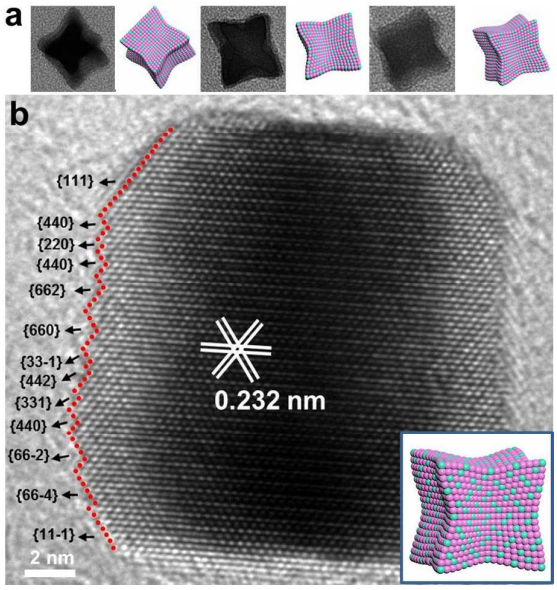

Figure S7. (a) TEM images and the projection models with different angles and (b) HRTEM image of Pd_3Pb CNCs. The inset in (b) is the 3D structure model of Pd_3Pb CNC.

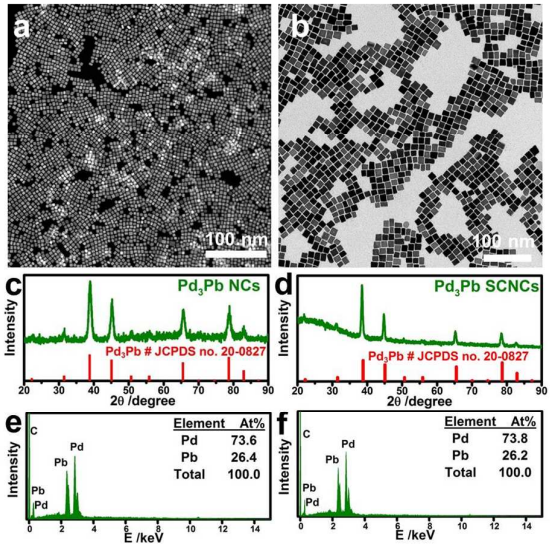

Figure S8. (a) STEM image, (c) PXRD pattern and (e) TEM-EDX of Pd_3Pb NCs. (b) TEM image, (d) PXRD pattern and (f) TEM-EDX of Pd_3Pb SCNCs.

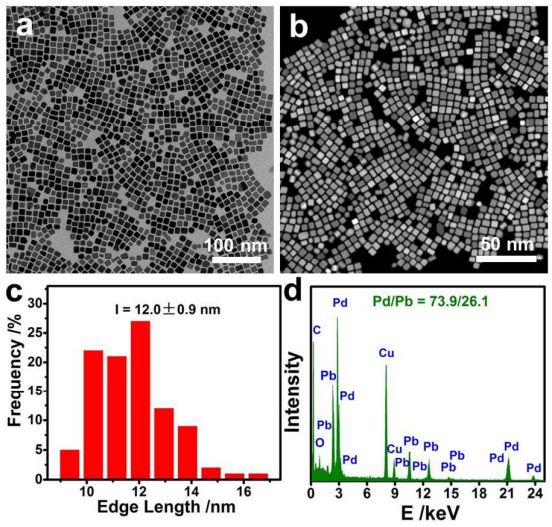

Figure S9. (a) TEM image, (b) STEM image, (c) edge length distribution and (d) SEM-EDX of Pd_3Pb NCs.

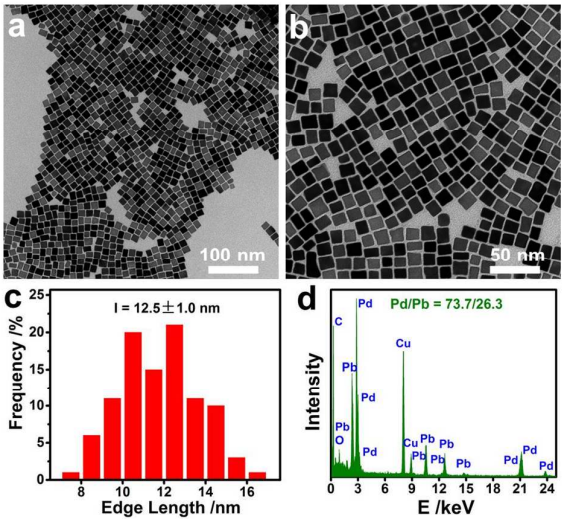

Figure S10. (a, b) TEM images, (c) edge length distribution and (d) SEM-EDX of Pd_3Pb SCNCs.

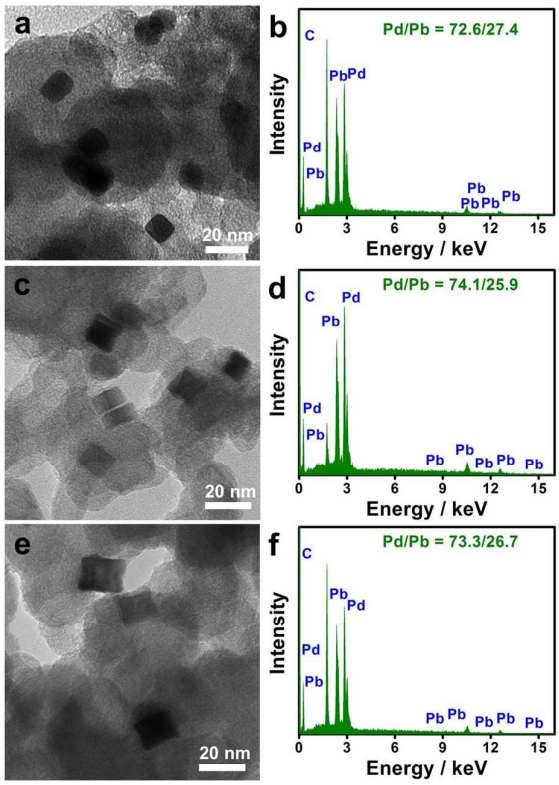

Figure S11. (a) TEM image and (b) SEM-EDX spectrum of Pd3Pb NCs/C. (c) TEM image and (d) SEM-EDX spectrum of Pd3Pb SCNCs/C. (e) TEM image and (f) SEM-EDX spectrum of Pd3Pb CNCs/C.

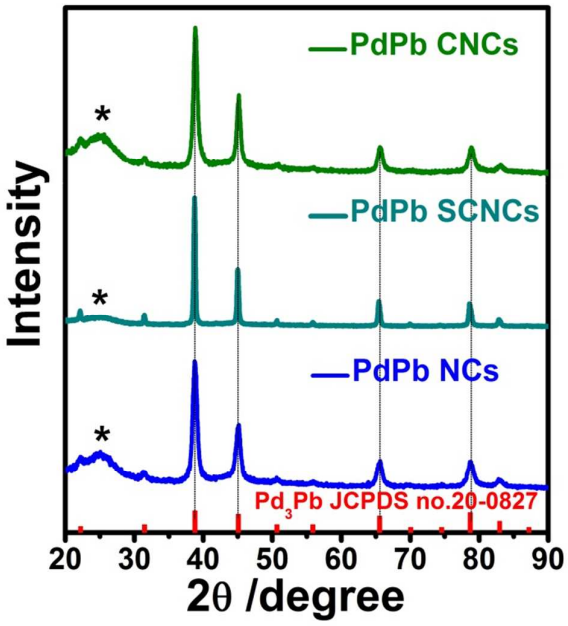

Figure S12. XRD patterns of 3 wt% Pd3Pb NCs/C, 3 wt% Pd3Pb SCNCs/C and 3 wt% Pd3Pb CNCs/C after calcining treatment. "*" notes the diffraction peak of C.

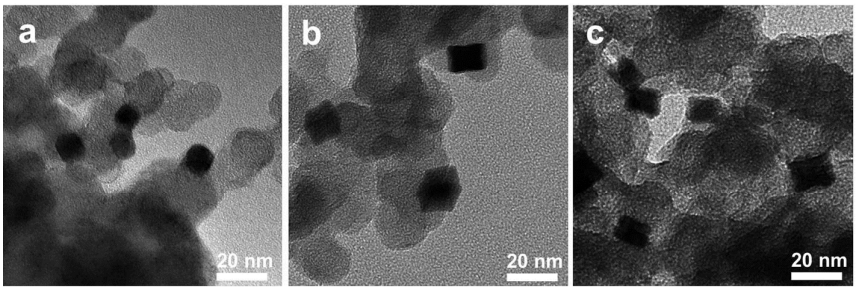

Figure S13. (a) TEM image of Pd3Pb NCs/C, (b) TEM image of Pd3Pb SCNCs/C and (c) TEM image of Pd3Pb CNCs/C after calcining treatment.

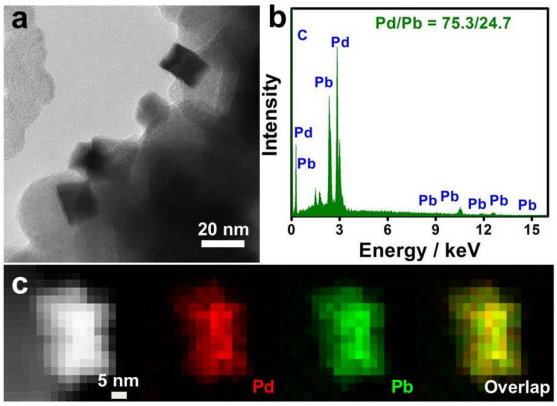

Figure S14. (a) TEM image, (b) SEM-EDX spectrum, and (c) HAADF-STEM image and elemental mappings of the Pd3Pb CNCs/C after stability tests.

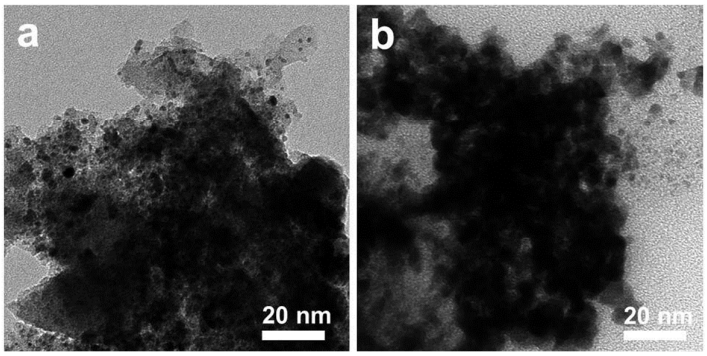

Figure S15. TEM images of 10% Pd/C (a) before and (b) after catalytic reaction.

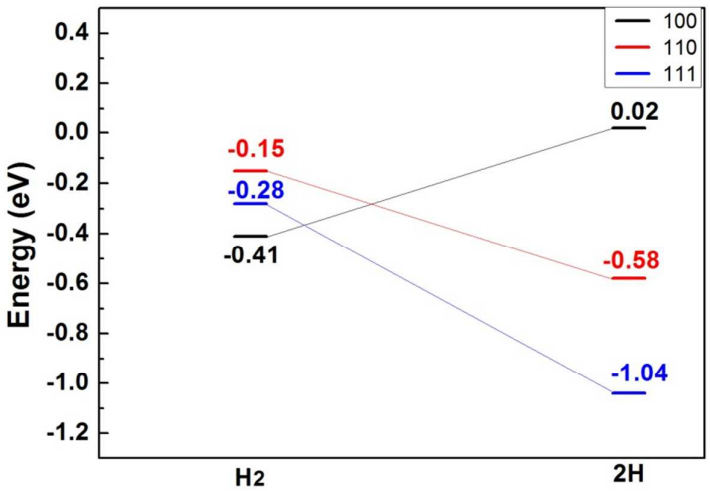

Figure S16. The energy of H_2 dissociation on (100) (110) and (111) surfaces of Pd_3Pb.

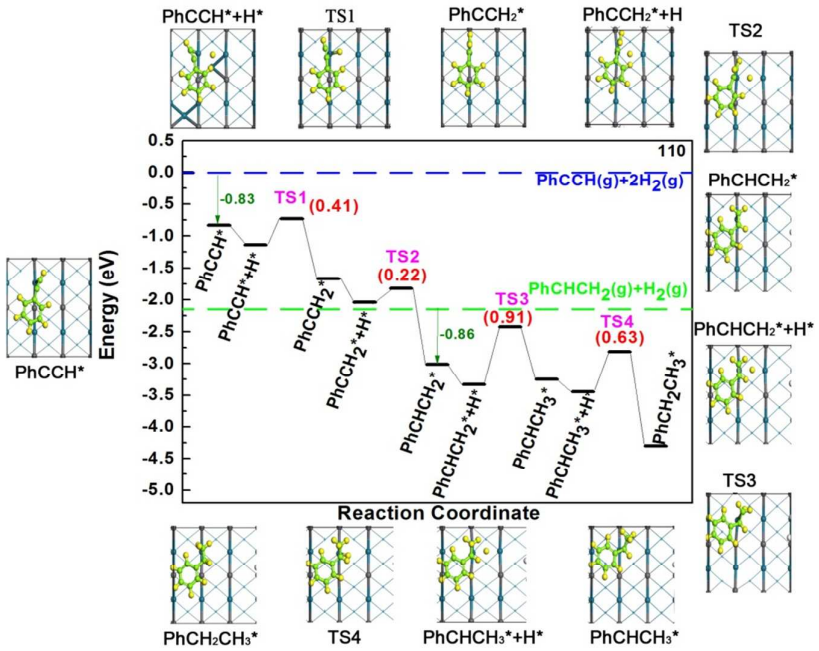

Figure S17. Step-by-step hydrogenation mechanism of phenylacetylene to phenylethane on the Pd_3Pb (110) surface. Numbers in the parentheses indicate the barriers of elementary steps; Pb, grey; Pd, blue; C, green; H, yellow.

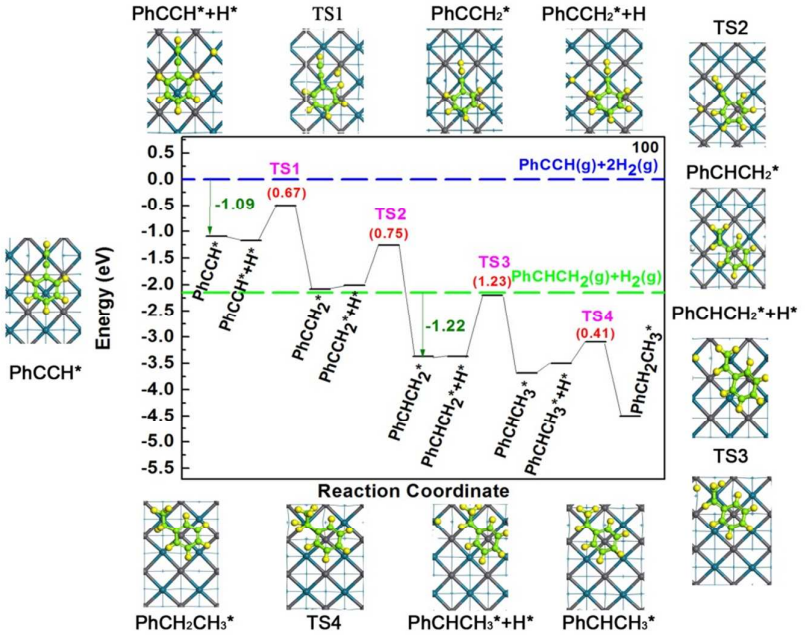

Figure S18. Step-by-step hydrogenation mechanism of phenylacetylene to phenylethane on the Pd_3Pb (100) surface. Numbers in the parentheses indicate the barriers of elementary steps; Pb, grey; Pd, blue; C, green; H,

yellow.

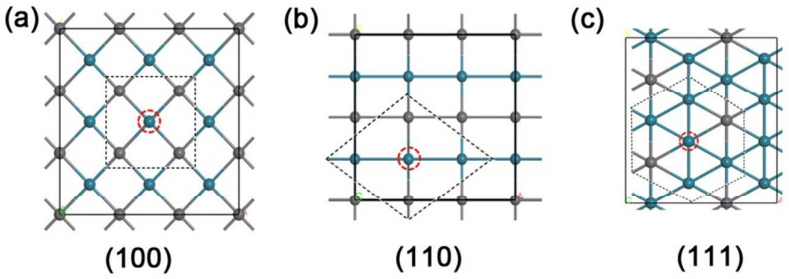

Figure S19. The atomic distribution of (100) (110) (111) surface of Pd_3Pb. The black dashed line includes the surrounding atoms with the central Pd atom in red dashed line.

Table S1. The concentration of Pd and Pb for 3 wt% Pd_3Pb NCs, 3 wt% Pd_3Pb SCNCs and 3 wt% Pd_3Pb CNCs.

	Pd wt%	Pb wt%
3 wt% Pd_3Pb NCs	3.07	1.01
3 wt% Pd_3Pb SCNCs	2.98	0.98
3 wt% Pd_3Pb CNCs	3.04	1.02

Table S2. XPS derived molar ratios (at%) and chemical states of 3.07 wt% Pd_3Pb NCs/C, 2.98 wt% Pd_3Pb SCNCs and 3.04 wt% Pd_3Pb CNCs/C.

Entry	**Catalyst**	**Pd** (at%)	**Pb** (at%)	**Pd($3d_{5/2}$) Binging Energy/eV**		**Pb($4f_{7/2}$) Binging Energy/eV**		**Pb/Pd ratio**
				Pd(0)	**Pd(II)**	**Pb(0)**	**Pb(II)**	
1	3.07 wt% Pd_3Pb NCs/C	73.3	26.7	336.0 (78.3%)	337.2 (21.7%)	137.4 (69.0%)	139.0 (31.0%)	0.364
2	2.98 wt% Pd_3Pb SCNCs/C	76.9	23.6	336.0 (77.5%)	337.5 (22.5%)	137.4 (77.5%)	139.1 (22.5%)	0.307
3	3.04 wt% Pd_3Pb CNCs/C	75.5	24.5	336.0 (88.5%)	337.3 (11.5%)	137.4 (65.4%)	138.9 (34.6%)	0.325

Table S3. Adsorption energies in eV determined by DFT for H_2 and H atom.

	$E_{ads}(H_2)$	E(H)
100	-0.41	0.01
110	-0.15	-0.29
111	-0.28	-0.52